Electrical and structural properties of Be- and Si-doped low-temperature-grown GaAs

N. Atique, E. S Harmon, J. C. P. Chang, J. M. Woodall, and M. R. Melloch[a]
School of Electrical Engineering, Purdue University, West Lafayette, Indiana 47907-1285

N. Otsuka
Department of Materials Science, Japan Advanced Institute of Science and Technology, Hokuriku, Nomigun, Ishikawa 923-12, Japan

Excess As is incorporated in GaAs grown at low substrate temperatures by molecular beam epitaxy. Excess As is distributed in the epilayer as defects and the material exhibits considerable strain. When annealed to moderate temperatures, the strain is seen to disappear and the excess As is now in the form of semimetallic clusters. It has been proposed that these As clusters form buried Schottky barriers with the GaAs matrix and are surrounded by spherical depletion regions. In this article, we examine the effects of doping on the material properties and compare our results to the buried Schottky barrier mode. Si-doped GaAs epilayers grown at 250 °C, with doping densities between 5×10^{17} and 5×10^{18} cm^{-3}, were annealed to temperatures between 700 and 1000 °C for 30 s. Be-doped GaAs epilayers grown at 250 °C, with doping densities between 5×10^{17} and 5×10^{19} cm^{-3}, were annealed to temperatures between 700 and 900 °C for 30 s. Using extensive Hall measurements and transmission electron microscopy, we observe that the As precipitates deplete the surrounding GaAs matrix. © *1995 American Institute of Physics.*

I. INTRODUCTION

Excess As is incorporated in GaAs grown by molecular beam epitaxy (MBE) at low substrate temperatures. The excess As is incorporated in the form of point defects, namely, As antisites and possibly As interstitials.[1] The total amount of the excess As present in the epilayer is dependent on the substrate temperature during MBE and decreases with increasing substrate temperature.[2,3] There is considerable strain in the material due to the excess As and it has been observed that this strain is relaxed with modest anneals.[1,4–5] Initial transmission electron microscope (TEM) observations of annealed low-temperature-grown (LTG) GaAs epilayers reported no obvious defects.[6] However, it is now known that after anneals of just 30 s at temperatures of 550 °C or higher, precipitation of the excess As occurs.[2,7–16] With scanning tunneling microscopy (STM), Feenstra et al.[17] have imaged the As antisites and detected an As antisite concentration of about 10^{20} cm^{-3} for the as-grown material. After annealing, As precipitates at a concentration of about 10^{17} cm^{-3} but no As antisites were detected with STM.[18] This means that the As antisite concentration was $<10^{17}$ cm^{-3} after the anneal. There is still a great deal of controversy surrounding the role of As precipitates versus residual defects in controlling the material properties of annealed LTG-GaAs.[19–24] The purpose of this study is to determine the role of the As precipitates in n- and p-doped LTG-GaAs.

The post-growth anneal temperature can be used to control the size and density of As precipitates in a GaAs matrix. Higher temperature anneals result in larger As clusters that are spaced further apart.[12,15] This is illustrated in Fig. 1. However, the total amount of the excess As in the epilayer is fixed by the substrate temperature during MBE.[2] The As clusters are semimetallic in nature and form buried Schottky barriers with the surrounding GaAs matrix.[18,19] Our study involves a comprehensive analysis of the other controlling factor we have over the structure of the As precipitates—doping. It has been shown that delta-doping,[11] p-n junctions,[12] doping type,[12,13,25] and doping concentration[12] can influence the coarsening of the As precipitates. It has also been shown that as one anneals LTG Si-doped GaAs at higher temperatures, Hall measurements indicate an increase in electron concentration.[26] In our experiments, we used a wide range of doping concentrations. The p-type epilayers were doped with Be to concentrations of 5×10^{17}, 1×10^{18}, 5×10^{18}, 1×10^{19}, and 5×10^{19} cm^{-3}. For the n-type epilayers, Si was the dopant and concentrations of 5×10^{17}, 1×10^{18}, and 5×10^{18} cm^{-3} were used.

Our objective in this study is to understand the nature of doped LTG-GaAs and to see how well the model of As precipitates as buried Schottky barriers corroborates our results. In order to do so, our samples were annealed to temperatures of 700, 800, 900, and 1000 °C for 30 s, yielding precipitates of various sizes. Detailed electrical and structural analyses were then performed. Hall measurements were made on the samples to observe how resistivity, carrier concentration, and mobility vary with anneal temperature. TEM analysis on the corresponding samples yield average values for the diameters and the density of the clusters. Using the model proposed by Warren et al.,[19] we are able to predict how the carrier concentration should change with anneal temperature. The Si-doped and Be-doped annealed LTG epilayers show very good agreement with the embedded Schottky barrier model. However, for the higher Be dopings, the carrier concentrations are lower than predicted by the embedded Schottky barrier model, indicating some compensation of the shallow acceptors by residual point defects.

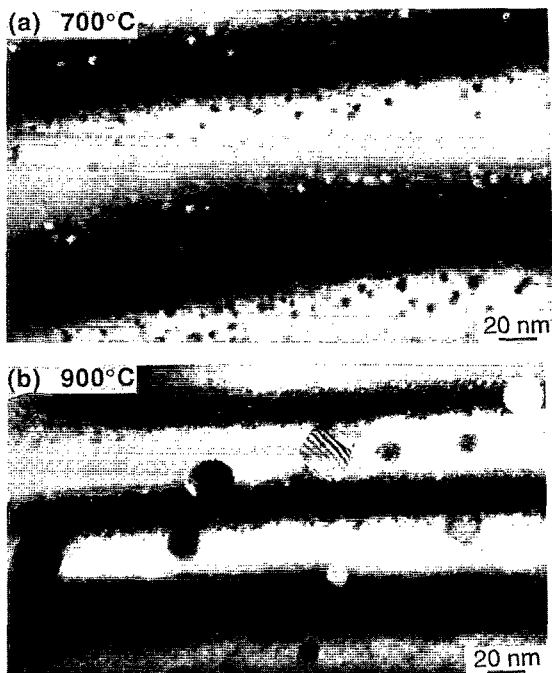[a] E-mail:melloch✒@ecn.purdue.edu

FIG. 1. Bright field image of a Be-doped LTG-GaAs epilayer annealed for 30 s at (a) 700 °C and (b) 900 °C.

II. EXPERIMENTAL

A. Film growth

The films used in our study were grown in a GEN II MBE system on 2 in. diameter undoped GaAs substrates. The substrates were degreased, etched for 1 m in a 60 °C solution of 5:1:1 H_2SO_4:H_2O_2:H_2O and placed in nonindium mounts. They were then loaded into a trolley and placed in the entry chamber of the MBE system where they were out-gassed for 2 h at 200 °C before being introduced into the buffer chamber of the MBE system. Liquid nitrogen was circulated through the radial vane and the cryoshrouds of the growth chamber starting 2 h before film growth. The sub-strates were outgassed at 350 °C for 1 h on a heater station in the buffer chamber immediately before being loaded into the growth chamber.

The As source used was the dimer As_2, which has been reported to be more efficient than the tetramer source As_4 for As incorporation in LTG-GaAs.[8] The growth rate was 1 μm/h and the beam equivalent pressure of As_2 to Ga was 20. Initially 0.5 μm of undoped GaAs was grown at a substrate temperature of 600 °C. Growth was stopped and the sub-strate temperature lowered to 250 °C followed by the growth of a 0.75 μm uniformly doped LTG epilayer. A series of samples with Si concentrations of 5×10^{17}, 1×10^{18}, 5×10^{18} cm^{-3} and Be concentrations of 5×10^{17}, 1×10^{18}, 5×10^{18}, 1×10^{19}, and 5×10^{19} cm^{-3} were grown. The Be and Si con-centrations were determined by Hall effect measurements on epilayers grown under normal growth conditions, that is, with no excess As in the epilayers. The Be-doped samples were then annealed with a proximity cap to 700, 800, and 900 °C for 30 s using an AG Associates automated rapid

thermal annealer (RTA). The Si-doped samples were an-nealed to the same temperatures as well as 1000 °C for 30 s.

B. TEM Analysis

TEM analysis was performed on a few of the annealed samples to seek trends in the sizes and densities of the As clusters with anneal temperature. [011] cross-sectional samples were prepared by the standard Ar ion thinning tech-nique and examined using a JEM 2000EX electron micro-scope. Arsenic precipitates surrounded by a perfect GaAs crystal were observed in all the samples. Moiré fringes were also visible in the As precipitates in all the samples. These indicate that the As precipitates are crystalline in nature, even after a 1000 °C, 30 s anneal. Quantitative analyses of the sizes and density of the As precipitates were then carried out using (111) bright-field images, as shown in Fig. 1 for the 5×10^{19} cm^{-3} Be-doped LTG-GaAs epilayer annealed to (a) 700 and (b) 900 °C. Sample thicknesses and subsequently volumes were determined from thickness contours. Cluster densities were calculated by counting the number of precipi-tates in a given volume. A few of the precipitates did not possess well-defined boundaries, but other contrasting fac-tors such as density, atomic number, structure factor, moiré fringes, and the lattice strain field around precipitates, aided in their identification. As a result, measured precipitate den-sities are very close to the actual values. Precipitate diam-eters were averaged over about 100 well-defined precipitates and the standard deviation, as a percent of the diameter, ranged from 15% to 30% of the average value.

The measured precipitate sizes and spacings are plotted versus anneal temperature in Fig. 2 for both the n- and p-doped material. The diameters of the precipitates ranged from about 50 to 250 Å. The precipitate densities ranged from 1×10^{15} to 1×10^{17} cm^{-3}. The spacing between precipi-tates (calculated from the density) ranged from about 200 to 1000 Å. It is clear that the As clusters are coarsening with higher anneal temperatures. The volume fraction of excess As, determined by TEM, was about 0.9% for the Si-doped material and about 0.6% for the Be-doped material, for all the different anneals. X-ray diffraction on a few of the an-nealed and as-grown materials was performed and the results of x-ray rocking curves showed no visible strain in the an-nealed material, indicating that most of the excess As was precipitated by the 700 °C, 30 s anneal. The as-grown mate-rial did exhibit considerable strain, equating to a peak sepa-ration of about 130 arcsec for the n-type material. At this point, it has not been determined why there is a difference in volume fraction of excess As between the Si- and Be-doped epilayers; it may be due to the surface atomic processes that are taking place during MBE.

TEM analysis revealed another interesting trend—higher doping levels resulted in smaller and more densely packed precipitates for a given anneal (see Fig. 2). This result will be discussed further in Sec. III.

C. Hall measurements

Electrical measurements were performed using a stan-dard Hall effect system. Van der Pauw samples with In con-tacts were used. For the annealed LTG-GaAs epilayers, the
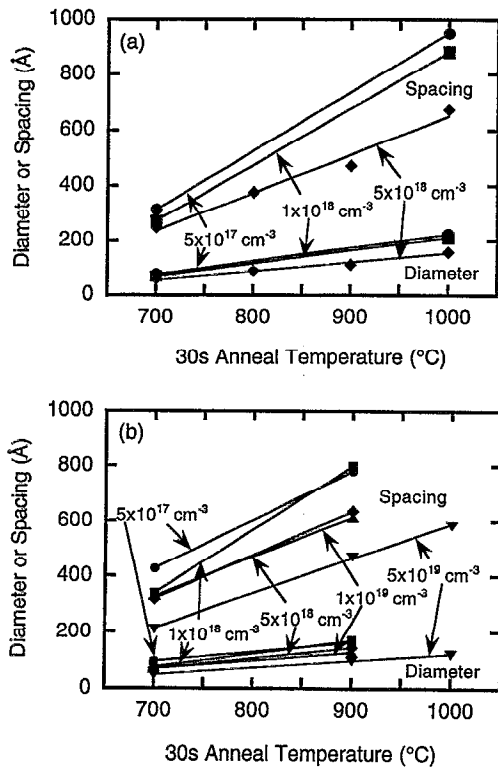
FIG. 2. Average cluster sizes and spacings as a function of anneal temperature for 30 s isochronal anneals of LTG-GaAs epilayers for (a) three different Si-doping levels and (b) five different Be-doping levels.

In contacts were alloyed at 400 °C for about 30 s to provide good ohmic contacts. The alloying temperature for the as-grown samples was 200 °C (less than the growth temperature) so as not to affect the samples. The electrical measurements are summarized in Tables I and II.

Figure 3 plots resistivity versus anneal temperature for both the Si- and Be-doped samples. Annealing the samples to 700 °C for 30 s results in high resistivity material due to the high concentration of As precipitates, as determined with

TABLE I. Resistivity, mobility, and carrier concentration of Si-doped epilayers measured by Hall effect.

Si concentration (cm^{-3})	Anneal temperature (°C)	Resistivity (Ω cm)	Mobility (cm^2/V s)	Carrier concentration n(cm^{-3})
5×10^{17}	as-grown	735	3.6	2.38×10^{15}
	700	38500	209.6	7.73×10^{11}
	800	13300	343.2	1.36×10^{12}
	900	1.78	547.6	6.39×10^{15}
	1000	0.172	1168.2	3.11×10^{16}
1×10^{18}	as-grown	1010	14.1	4.38×10^{14}
	700	33900	888	2.07×10^{11}
	800	0.354	613.2	2.88×10^{16}
	900	0.0307	1153.8	1.76×10^{17}
	1000	0.0137	1669	2.73×10^{17}
5×10^{18}	as-grown	1290	9.6	5.01×10^{14}
	700	334	332.2	5.62×10^{13}
	800	0.0355	868.4	2.03×10^{17}
	900	0.00713	1363.5	6.42×10^{17}
	1000	0.00485	1145.9	1.12×10^{18}

TABLE II. Resistivity, mobility, and carrier concentration of Be-doped epilayers measured by Hall effect.

Be concentration (cm^{-3})	Anneal temperature (°C)	Resistivity (Ω cm)	Mobility (cm^2/V s)	Carrier concentration p/n (cm^{-3})
5×10^{17}	as-grown	359	1.1	1.62×10^{16} (n)
	700	22600	460.5	5.99×10^{11} (n)
	800	2175	...	...
	900	5.53	48.2	2.34×10^{16}
1×10^{18}	as-grown	353	...	...
	700	24300	...	...
	800	8630	44.6	1.62×10^{13}
	900	0.239	68.4	3.82×10^{17}
5×10^{18}	as-grown	176	...	...
	700	21100	89.1	3.32×10^{12}
	800	1050	...	...
	900	0.032	60.6	3.22×10^{18}
1×10^{19}	700	18800	166.3	2.00×10^{12} (n)
	800	19.6	2.4	1.33×10^{17}
	900	0.0188	49.2	6.75×10^{18}
5×10^{19}	as-grown	16.4	...	...
	700	2570	193.9	1.25×10^{13}
	800	0.00591	28.7	3.68×10^{19}
	900	0.00262	48.6	4.90×10^{19}

TEM, which depletes the epilayer of free carriers. Figure 3 also shows that the resistivity goes down with higher temperature (800 to 1000 °C) anneals. This is consistent with the TEM analysis which shows the precipitates to be coarsening with higher temperature anneals. When the As precipitates coarsen to the point that the depletion regions no longer overlap, the carrier concentration goes up rapidly and the
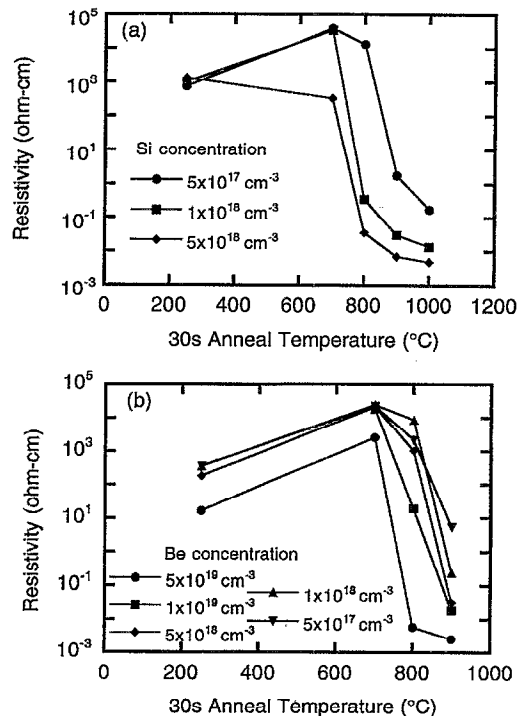

FIG. 3. Resistivity as a function of anneal temperature for 30 s isochronal anneals of LTG-GaAs epilayers for (a) three different Si doping levels and (b) five different Be-doping levels.
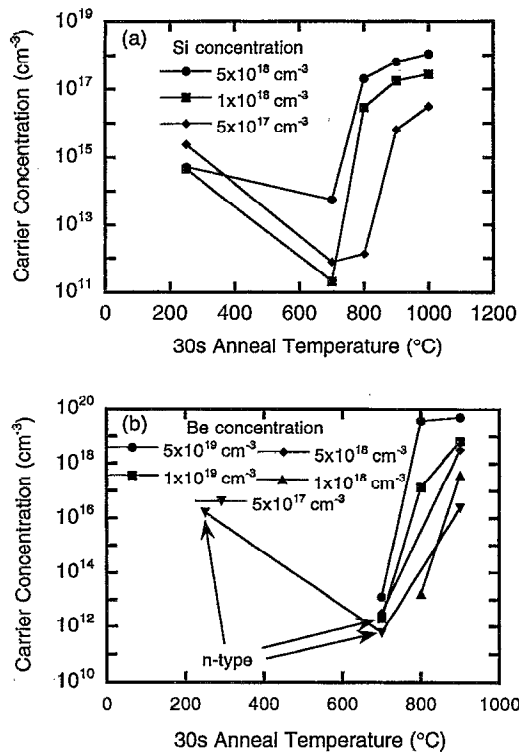
FIG. 4. Carrier concentration as a function of anneal temperature for 30 s isochronal anneals of LTG-GaAs epilayers for (a) three different Si-doping levels and (b) five different Be-doping levels.

FIG. 6. Schottky barrier model proposed by Warren et al.

material turns conducting. Resistivities as low as 2.6×10^{-3} Ω cm are obtained. Electrical measurements of the high resistivity samples shown in Fig. 3 are limited by substrate conduction. Also note that what appears to be an anneal temperature of 250 °C is just the growth temperature and those points represent the resistivity of the as-grown material.

The carrier concentrations and mobilities—as determined from Hall measurements—are shown in Figs. 4 and 5, respectively. Figure 4 shows that carrier concentration increases with higher temperature anneals confirming the fact that the coarsening of the precipitates causes the depletion
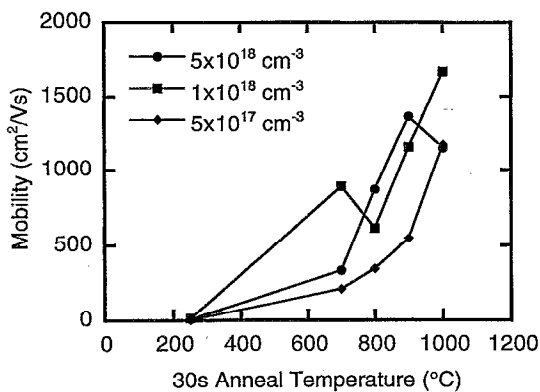

FIG. 5. Mobility as a function of anneal temperature for 30 s isochronal anneals for the Si-doped LTG-GaAs epilayers.
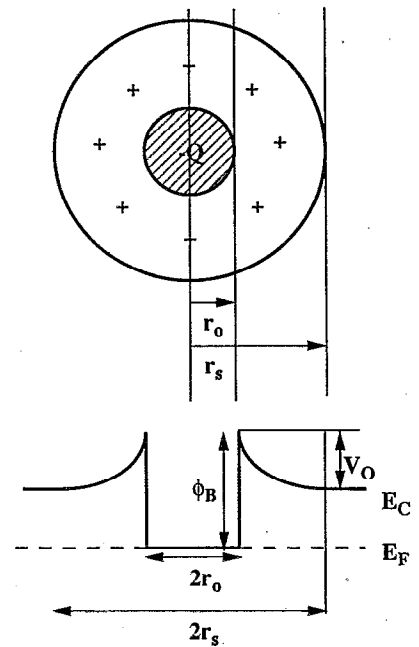
regions to no longer overlap and allow plenty of free carrier motion. This effect is also observed in Fig. 5, which shows that the mobility of the carriers increases with higher temperature anneals and mobilities as high as 1669 cm^2/V s are obtained. (Note that mobilities that look like zero in Fig. 5 are actually in the range from 1 to 15 cm^2/V s; see Table I.) Mobility data for the Be-doped material are not plotted since some of the mobilities were so low that accurate Hall measurements were not possible. This also explains the fewer data points in Fig. 4(b). Also seen in Fig. 4(b) is the occurrence of n-type conductivity for the as-grown and some of the lower temperature annealed material; similar observations have been reported by others.[27,28]

III. DISCUSSION

From photoreflectance,[26] STM,[18] and photoemission[23] spectroscopy, the As precipitate to GaAs Schottky barrier height, ϕ_B, has been measured to be approximately 0.7 eV. Figure 6 shows the model and band structure of an As precipitate surrounded by its spherical depletion region. In this model, the As precipitate forms a Schottky barrier with the GaAs matrix analogous to a planar Schottky barrier. By solving Poisson's equation, the built-in potential V_0 in Fig. 6—determined from the doping level of the material—is related to the As precipitate radius r_0 and the depletion radius r_s by[19]

$$V_0 = -(qN_D/6\epsilon)[(2r_s^3/r_0) + r_0^2 - 3r_s^2], \qquad (1)$$

where N_D is the doping density and ϵ is the permittivity of the semiconductor matrix. This equation allows the calculation of the depletion radius for each of our samples, which enables an estimation of the free carrier concentration from the fraction of material depleted. The expected free carrier
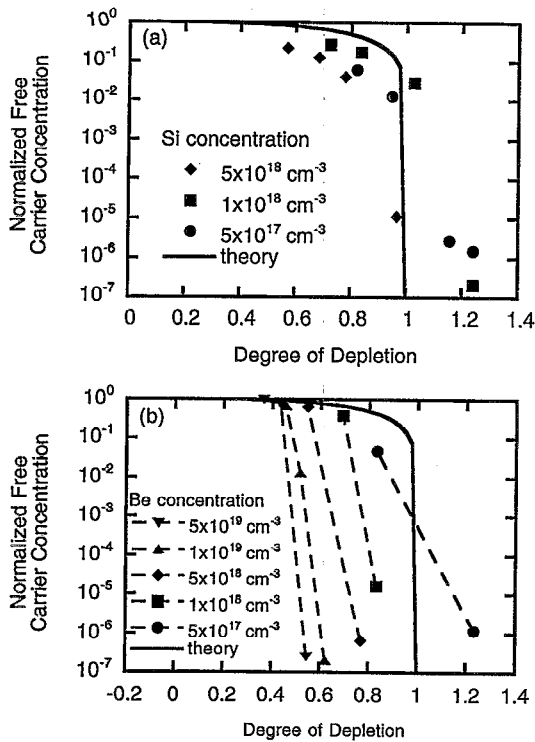
FIG. 7. Normalized carrier concentration vs degree of depletion for (a) three different Si-doping levels and (b) five different Be-doping levels. Degree of depletion is $2r_s/d$, where r_s is the depletion sphere radius and d is the distance between precipitates.

concentration N_f for each sample is related to the doping density N_D, the depletion radius r_s, and the distance between precipitates d by

$$N_f = N_D[1-(2r_s/d)^3]. \qquad (2)$$

Plotted in Fig. 7 is normalized free carrier concentration N_f/N_D versus degree of depletion. Degree of depletion is the extent of the depletion region overlap and is given by $(2r_s)/d$, where d is the spacing between precipitates. A degree of depletion of 1 means the depletion regions are touching and a degree of depletion of 0.5 means only half the distance between precipitates is depleted. The theoretical curve calculated using Eqs. (1) and (2) is illustrated by the solid curve in Fig. 7. The experimental free carrier concentrations (from Hall measurements) assumes conduction through the entire volume of each sample. However, when some of the material is depleted by As precipitates, the volume available for conduction is less, and so actual carrier concentrations are higher in the undepleted regions. The experimental data points are scattered very close to the theoretical curve in Fig. 7(a) for the Si-doped material, indicating that the embedded Schottky barrier model accounts for the observed results. The existence of a few experimental data points to the right of a degree of depletion of 1, in Fig. 7(a), is due to our use of the depletion approximation in Eq. (1) and because there is still some contribution of carriers from unpinched off material not accounted for in Eq. (2).

The normalized hole concentrations as a function of depletion overlap are shown in Fig. 7(b). The 5×10^{17} cm^{-3}

Be-doped sample follows the predictions of the embedded Schottky barrier model (solid curve), but as the Be-doping concentration increases, the experimental normalized hole concentrations shift to the left of the theoretical curve. This result is expected based on previous observations of As precipitation in p-doped LTG-GaAs.[12] As-grown p-doped LTG-GaAs is at a lower free energy than as-grown n-doped LTG-GaAs because the excess As, in the form of deep donor As antisites, will compensate the p-doped LTG-GaAs. Therefore, in p-type LTG-GaAs, the excess As does not precipitate as readily as in n-doped LTG-GaAs. Also, the higher the p-doping concentration the less readily does the As precipitate, because a larger fraction of the As antisites are ionized and compensating the shallow p-dopants. Furthermore, for a given anneal temperature, as the n- or p-doping concentration increases the As clusters are smaller and denser, as seen in Fig. 2. This is due to the crystal trying to minimize its free energy by driving the Fermi level to midgap, which requires a higher As precipitate density as the doping increases.

IV. SUMMARY

The effect of anneal on the structure and electronic properties of n- and p-doped LTG-GaAs has been studied. The electronic properties of the as-grown LTG-GaAs epilayers are controlled by point defects. As the material is annealed, the excess As precipitates and plays an increased role in controlling the electronic properties of the material, whereas the role of point defects decreases. For sufficient anneal, the embedded Schottky barrier model for the As precipitates adequately explains the electronic properties of annealed doped LTG-GaAs epilayers.

With an anneal of 700 °C for 30 s, there is a large increase in the resistivity of the doped LTG-GaAs epilayers. This increase in resistivity is due to the As precipitates depleting the GaAs matrix of free carriers. With higher anneals, the As precipitates coarsen, the depletion regions surrounding the As precipitates no longer overlap, and the conductivity approaches that expected from the n- or p-doping. For high Be concentrations, there is some compensation of the shallow acceptors due to residual As antisites, leading to depletion of the epilayer by the As precipitates at lower As precipitate concentrations than expected. Also, for a given anneal temperature, a higher n- or p-doping concentration results in a higher density and a smaller diameter for the As precipitates due to the crystal minimizing its free energy.

ACKNOWLEDGMENTS

[1] M. Kaminska, E. R. Weber, Z. Liliental-Weber, R. Leon, and Z. U. Rek, J. Vac. Sci. Technol. B **7**, 710 (1989).
[2] K. Mahalingam, N. Otsuka, M. R. Melloch, J. M. Woodall, and A. C. Warren, J. Vac. Sci. Technol. B **9**, 2328 (1991).
[3] Z. Liliental-Weber, A. Claverie, J. Washburn, F. Smith, and R. Calawa, Appl. Phys. A **53**, 141 (1991).
[4] C. R. Wie, K. Xie, D. C. Look, K. R. Evans, and C. E. Stutz, Mater. Res. Soc. Sym. Proc. **198**, 178 (1991).

J. Appl. Phys., Vol. 77, No. 4, 15 February 1995

Atique *et al.* 1475

[5] R. J. Matyi, M. R. Melloch, and J. M. Woodall, Appl. Phys. Lett. **60**, 2642 (1992).

[6] M. Kaminska, Z. Liliental-Weber, E. R. Weber, T. George, J. B. Kortright, F. W. Smith, B-Y. Tsauer, and A. R. Calawa, Appl. Phys. Lett. **54**, 1881 (1989).

[7] M. R. Melloch, N. Otsuka, J. M. Woodall, A. C. Warren, and J. L. Freeouf, Appl. Phys. Lett. **57**, 1531 (1990).

[8] M. R. Melloch, K. Mahalingam, N. Otsuka, J. M. Woodall, and A. C. Warren, J. Cryst. Growth **111**, 39 (1991).

[9] Z. Liliental-Weber, G. Cooper, R. Mariella, Jr., and C. Kocot, J. Vac. Sci. Technol. B **9**, 2323 (1991).

[10] K. Mahalingam, N. Otsuka, M. R. Melloch, and J. M. Woodall, Appl. Phys. Lett. **60**, 3253 (1992).

[11] M. R. Melloch, N. Otsuka, K. Mahalingam, C. L. Chang, P. D. Kirchner, J. M. Woodall, and A. C. Warren, Appl. Phys. Lett. **61**, 177 (1992).

[12] M. R. Melloch, N. Otsuka, K. Mahalingam, C. L. Chang, J. M. Woodall, G. D. Pettit, P. D. Kirchner, F. Cardone, A. C. Warren, and D. D. Nolte, J. Appl. Phys. **72**, 3509 (1992).

[13] J. P. Ibbetson, J. S. Speck, A. C. Gossard, and U. K. Mishra, Appl. Phys. Lett. **62**, 169 (1993).

[14] J. P. Ibbetson, J. S. Speck, A. C. Gossard, and U. K. Mishra, Appl. Phys. Lett. **62**, 2209 (1993).

[15] M. R. Melloch, J. M. Woodall, N. Otsuka, K. Mahalingam, C. L. Chang, and D. D. Nolte, Mater. Sci. Eng. B **22**, 31 (1993).

[16] T. M. Cheng, A. Chin, C. Y. Chang, M. F. Huang, K. Y. Hsieh, and J. H. Huang, Appl. Phys. Lett. **64**, 1546 (1994).

[17] R. M. Feenstra, J. M. Woodall, and G. D. Pettit, Mater. Sci. Forum **143-147**, 1311 (1994).

[18] R. M. Feenstra, A. Vaterlaus, J. M. Woodall, and G. D. Pettit, Appl. Phys. Lett. **63**, 2528 (1993).

[19] A. C. Warren, J. M. Woodall, J. L. Freeouf, D. Grischkowsky, D. T. McInturff, M. R. Melloch, and N. Otsuka, Appl. Phys. Lett. **57**, 1331 (1990).

[20] A. K. Verma, J. Tu, J. S. Smith, H. Fujioka, and E. R. Weber, J. Electron. Mater. **22**, 1417 (1993).

[21] J. P. Ibbetson, J. S. Speck, N. X. Nguyen, A. C. Gossard, and U. K. Mishra, J. Electron. Mater. **22**, 1421 (1993).

[22] Z.-Q. Fang and D. C. Look, J. Electron. Mater. **22**, 1429 (1993).

[23] D. T. McInturff, J. M. Woodall, A. C. Warren, N. Braslau, G. D. Pettit, P. D. Kirchner, and M. R. Melloch, Appl. Phys. Lett. **60**, 448 (1992).

[24] N. D. Jager, A. K. Verma, P. Dreszer, N. Newman, Z. Liliental-Weber, M. Van Schilfgaarde, and E. R. Weber, J. Electron. Mater. **22**, 1499 (1993).

[25] C. L. Chang, K. Mahalingam, N. Otsuka, M. R. Melloch, and J. M. Woodall, J. Electron. Mater. **22**, 1413 (1993).

[26] A. C. Warren, J. M. Woodall, P. D. Kirchner, X. Yin, F. Pollak, M. R. Melloch, N. Otsuka, and K. Mahalingam, Phys. Rev. B **46**, 4617 (1992).

[27] D. E. Bliss, W. Walukiewicz, J. W. Ager, III, E. E. Haller, K. T. Chan, and S. Tanigawa, J. Appl. Phys. **71**, 1699 (1992).

[28] S. O'Hagan and M. Missous, J. Appl. Phys. **75**, 7835 (1994).